RESEARCH   **Open Access**

Metabolic engineering of *Komagataella phaffii* for enhanced 3-hydroxypropionic acid (3-HP) production from methanol

Sílvia Àvila-Cabré[1], Joan Albiol[1] and Pau Ferrer[1*]

Abstract

Background Bioconversion of methanol derived from CO_2 reduction into value-added chemicals provides a unique approach for mitigating global warming and reducing fossil fuels dependence. Production of 3-hydroxypropionic acid (3-HP), a key building block for the development of biobased products such as acrylates and 1,3-propanediol, has been successfully achieved using methanol as the sole carbon and energy source in the methylotrophic yeast *Komagataella phaffii* (syn. *Pichia pastoris*). However, challenges remain in meeting commercially relevant concentrations, yields and productivities of 3-HP, prompting further strain optimization. In the present study, we have combined metabolic engineering strategies aiming at increasing metabolic precursors supply and redirecting carbon flux towards 3-HP production.

Results A combinatorial metabolic engineering strategy targeting precursors supply and 3-HP export was applied to the original 3-HP producing *K. phaffii* strain harboring the synthetic β-alanine pathway and a mutated NADP-dependent formate dehydrogenase from *Pseudomonas* sp. 101 (PseFDH(V9)). To do so, several genes encoding enzymes catalyzing reactions immediately upstream of the β-alanine pathway were overexpressed to enhance precursors availability. However, only the overexpression of the pyruvate carboxylase *PYC2* gene significantly increased the 3-HP yield on biomass ($Y_{P/X}$) in small-scale cultivations. Co-overexpression of *PYC2* and the lactate permeases *ESBP6* and *JEN1* genes led to a 55% improvement in 3-HP titer and product yield in methanol deep-well plate cultures compared to the reference strain, mostly due to Esbp6 activity, proving its effectiveness as a 3-HP transporter. Deletion of the native formate dehydrogenase gene *FDH1* did not increase methanol flux entering the assimilatory pathway. Instead, knockout strains showed severe growth defects due to toxic intermediates accumulation. Co-expression of the PseFDH(V9) encoding gene in these strains failed to compensate for the loss of the native *FDH*. The strain combining *PYC2*, *ESBP6*, and *JEN1* overexpression was further tested in fed-batch cultures at pH 5, achieving a 3-HP concentration of 27.0 g l^{-1}, with a product yield of 0.19 g g^{-1}, and a volumetric productivity of 0.56 g l^{-1} h^{-1} for the methanol feeding phase of the cultivations. These results represent a 42% increase in final concentration and over 20% improvement in volumetric productivity compared to the original 3-HP-producing strain. Furthermore, bioreactor-scale cultivations at pH 3.5 revealed increased robustness of the strains overexpressing monocarboxylate transporters.

*Correspondence:
Pau Ferrer
Pau.Ferrer@uab.cat

Full list of author information is available at the end of the article

Conclusions Our results point out the potential of lactate transporters to efficiently drive 3-HP export in *K. phaffii*, leading to higher titers, yields, and productivities, even at lower pH conditions.

Keywords 3-hydroxypropionic acid, *Pichia pastoris*, *Komagataella phaffii*, Methanol, ß-alanine pathway, Metabolic engineering, Lactate transporters

Background

The valorization of industrial CO_2 effluents has the potential to play a crucial role in addressing climate crisis and advancing towards a more sustainable production cycle. CO_2 can be reduced with hydrogen to produce methanol, a sustainable carbon and energy source [1, 2]. Bioconversion of this low-cost one-carbon (C1) feedstock into valuable chemicals not only has the potential to reduce reliance on fossil fuels but also to help mitigate climate change, representing a promising approach within the framework of a circular economy [3–5].

3-Hydroxypropionic (3-HP) acid is a key building block that can be used as a precursor to produce several valuable chemicals, including acrylates, 1,3-propanediol, propiolactone, malonic acid, and hydroxyamides. Moreover, as a homopolymer or when integrated into other biopolymers, 3-HP has the potential to replace petrochemistry-based polymers, offering a sustainable alternative for the synthesis of advanced materials [6, 7]. In 2004, the US Department of Energy (DOE) ranked this C3 organic acid in a significant third position among the top twelve biobased value-added chemicals [8]. An updated version of this ranking was published six years later, where 3-HP was included again [9]. Despite its potential, chemical synthesis of 3-HP faces several challenges, including the high cost of raw materials, low yields, complex reaction steps, and the involvement of toxic, noxious, or carcinogenic compounds [10]. Several microorganisms naturally synthesize 3-HP, either as an intermediate or as a product, through different metabolic pathways and diverse substrates such as glycerol, glucose, CO_2 or uracil. The most studied pathways include the coenzyme B_{12}-dependent glycerol pathways (both CoA-dependent and CoA-independent) and the malonyl-CoA reductase pathway, which is part of the 3-hydroxypropionate/malyl-CoA and 3-hydroxypropionate/4-hydroxybutyrate autotrophic cycles [11, 12]. However, significant byproduct formation and suboptimal yields and productivities still hinder the commercial viability of biological 3-HP production. To overcome these issues, metabolic engineering of both natural and non-natural producers has been investigated.

Among bacterial hosts, *Escherichia coli* and *Klebsiella pneumoniae* have been the most widely used for 3-HP production via the glycerol pathway [13]. These bacteria have produced by far the highest reported 3-HP titers (76.2 and 102.6 g l^{-1}, respectively) and volumetric productivities (1.89 and 1.07 g l^{-1} h^{-1}, respectively) [14, 15]. Several yeast species have also been engineered

to produce 3-HP, primarily through the introduction of the malonyl-CoA reductase pathway and the synthetic β-alanine pathway [16]. The bifunctional malonyl-CoA reductase from *Chloroflexus aurantiacus* (MCR_{Ca}) has been successfully expressed in *Saccharomyces cerevisiae* [17, 18], *Schizosaccharomyces pombe* [19, 20], and *Komagataella phaffii* (syn. *Pichia pastoris*), achieving the highest volumetric productivity reported so far in yeast (0.712 g l^{-1} h^{-1}) [21]. Additionally, the synthetic β-alanine pathway has been engineered into *S. cerevisiae* [22, 23], and subsequent bioprocess optimization enabled a final concentration of 27 g l^{-1}, with a product yield on glucose of 0.26 g g^{-1} [24]. Recently, the β-alanine pathway has been targeted to mitochondria in *S. cerevisiae*, leading to higher 3-HP production compared to the cytoplasmic pathway [25]. Interestingly, yeasts can withstand a pH as low as 3 [26, 27], which is more than 1 unit below the pKa of 3-HP (4.51) [28]. In these circumstances, the undissociated form of 3-HP is the most abundant fraction in the solution, lowering costs of downstream processing [29]. Therefore, yeasts stand as promising cell factories for 3-HP production.

Of particular interest is the methylotrophic yeast *K. phaffii*, which shows a distinct ability to grow on methanol as the sole carbon and energy source, making it an attractive cell factory to produce high-value-added chemicals from this low-cost and renewable substrate [30]. Moreover, methanol is a highly reduced carbon source ($γ = 6.0$), whose oxidation provides more redox equivalents than most sugars, potentially becoming a competitive substrate for the synthesis of highly reduced compounds such as terpenoids [31, 32], and fatty acids and their derivatives [33, 34]. In addition, recent studies have demonstrated *K. phaffii*'s ability to produce different organic acids from methanol as sole carbon source, including malic acid [35], D-lactic acid [36], itaconic acid [37], and 3-HP [38]. Recently, we have successfully engineered *K. phaffii* for 3-HP production from methanol by implementing the β-alanine pathway [39]. Specifically, we expressed the genes coding for a β-alanine-pyruvate aminotransferase from *Bacillus cereus* ($BAPAT_{Bc}$), a 3-hydroxypropionate dehydrogenase from *E. coli* ($YDFG_{Ec}$), and two copies of an aspartate-1-decarboxylase from *Tribolium castaneum* ($PAND_{Tc}$), obtaining a 3-HP-producing base strain (PpCβ21) that produced up to 21.4 g l^{-1} of 3-HP in methanol fed-batch cultures, with a yield of 0.15 g g^{-1} and a volumetric productivity of 0.48 g l^{-1} h^{-1}. Additional redox engineering of this strain

Table 1 List of plasmids and strains used in this study

Plasmids/Strains	Modules/Genotype	Reference
Plasmids		
BB1_12_pDAS1	P_{DAS1}, KanR$^+$	[57]
BB1_12_pDAS2	P_{DAS2}, KanR$^+$	
BB1_12_SHB17	P_{SHB17}, KanR$^+$	
BB1_23	Ø, KanR$^+$	
BB1_34_RPS3tt	RPS3tt, KanR$^+$	
BB1_34_ScCYC1tt	ScCYC1tt, KanR$^+$	
BB2_BC	Ø, AmpR$^+$	
BB1_23_AAT2	AAT2$^+$, *K. phaffii* gene encoding cytosolic aspartate aminotransferase Aat2	This work
BB1_23_SpeAspDH	aspDH$^+$, *S. proteamaculans* codon-optimized gene encoding aspartate dehydrogenase AspDH	
BB1_23_PYC2	PYC2$^+$, *K. phaffii* codon-optimized gene encoding pyruvate carboxylase Pyc2	
BB1_23_JEN1	JEN1$^+$, *K. phaffii* gene encoding putative lactate transporter Jen1	
BB1_23_ScESBP6	ESBP6$^+$, *S. cerevisiae* gene encoding monocarboxylate permease Esbp6	
BB1_23_PseFDH(V9)	fdh$^+$, *Pseudomonas* sp. (strain 101) gene encoding FDH$^+_{Pse}$(V9)$_{(A199G/D222Q/S381V/C256A/H380K)}$	[39]
BB2_BC_AAT2	P_{DAS1}-AAT2-RPS3tt	This work
BB2_BC_SpeAspDH	P_{DAS1}-AspDH$_{Spe}$-RPS3tt	
BB2_BC_PYC2	P_{SHB17}-PYC2-RPS3tt	
BB2_BC_JEN1	P_{DAS2}-JEN1-ScCYC1tt	
BB2_BC_ScESBP6	P_{DAS1}-ESBP6$_{Sc}$-ScCYC1tt	[39]
BB2_BC_PseFDH(V9)	P_{FDH1}-FDH(V9)$_{Pse}$-TDH3tt	[52]
BB3nK_ext_AD	Ø, KanR$^+$	This work
BB3nK_ext_AD_AAT2	5'-HR_P_{DAS1}-AAT2-RPS3tt_3'-HR(pENO1^{UP})	
BB3nK_ext_AD_SpeAspDH	5'-HR_P_{DAS1}-AspDH$_{Spe}$-RPS3tt_3'-HR(pENO1^{UP})	
BB3nK_ext_AD_PYC2	5'-HR_P_{SHB17}-PYC2-RPS3tt_3'-HR(AOX1tt$_{DOWN}$)	
BB3nK_ext_AD_JEN1	5'-HR_P_{DAS2}-JEN1-ScCYC1tt_3'-HR(GUT1tt$_{DOWN}$) 5'-HR_P_{DAS2}-JEN1-ScCYC1tt_3'-HR(pOPT1-1^{UP})	
BB3nK_ext_AD_ScESBP6	5'-HR_P_{DAS1}-ESBP6$_{Sc}$-ScCYC1tt_3'-HR(GUT1tt$_{DOWN}$) 5'-HR_P_{DAS1}-ESBP6$_{Sc}$-ScCYC1tt_3'-HR(pENO1^{UP})	[39]
BB3nK_ext_AD_PseFDH(V9)	5'-HR_P_{FDH1}-FDH(V9)$_{Pse}$-TDH3tt_3'-HR(pAOX1^{UP})	[52]
BB3cN_pGAP_23*_pLAT1_Cas9	P_{GAP}- Ø_P_{LAT1}_Cas9, NrsR$^+$	This work
BB3cN_pGAP_gRNA1(pENO1^{UP})_pLAT1_Cas9	P_{GAP}- gRNA1(P_{ENO1}^{UP})_P_{LAT1}_Cas9, NrsR$^+$	
BB3cN_pGAP_gRNA2(pENO1^{UP})_pLAT1_Cas9	P_{GAP}- gRNA2(P_{ENO1}^{UP})_P_{LAT1}_Cas9, NrsR$^+$	
BB3cN_pGAP_gRNA1(AOX1tt$_{DOWN}$)_pLAT1_Cas9	P_{GAP}- gRNA1(AOX1tt$_{DOWN}$)_P_{LAT1}_Cas9, NrsR$^+$	
BB3cN_pGAP_gRNA1(GUT1tt$_{DOWN}$)_pLAT1_Cas9	P_{GAP}- gRNA1(GUT1tt$_{DOWN}$)_P_{LAT1}_Cas9, NrsR$^+$	
BB3cN_pGAP_gRNA2(GUT1tt$_{DOWN}$)_pLAT1_Cas9	P_{GAP}- gRNA2(GUT1tt$_{DOWN}$)_P_{LAT1}_Cas9, NrsR$^+$	
BB3cN_pGAP_gRNA1(pOPT1-1^{UP})_pLAT1_Cas9	P_{GAP}- gRNA1(P_{OPT1-1}^{UP})_P_{LAT1}_Cas9, NrsR$^+$	
BB3cN_pGAP_gRNA2(ΔFDH1)_pLAT1_Cas9	P_{GAP}- gRNA2(ΔFDH1)_P_{LAT1}_Cas9, NrsR$^+$	
BB3cN_pGAP_gRNA1(pAOX1^{UP})_pLAT1_Cas9	P_{GAP}- gRNA1(P_{AOX1}^{UP})_P_{LAT1}_Cas9, NrsR$^+$	[39]

Table 1 (continued)

Plasmids/Strains	Modules/Genotype	Reference
***K. phaffii* strains**		
PpCβ21	$2\times(P_{AOX1}\_PAND_{Tc}) + P_{FDH1}\_BAPAT_{Bc} + P_{POR1}\_YDFG_{Ec}$	[39]
PpCβ21-P	$+ P_{FDH1}\_FDH(V9)_{Pse}$	This work
PpCβ21-A	$+ P_{DAS1}\_AAT2$	
PpCβ21-D	$+ P_{DAS1}\_AspDH_{Spe}$	
PpCβ21-Y	$+ P_{SHB17}\_PYC2$	
PpCβ21-YA	$+ P_{DAS1}\_AAT2$	
PpCβ21-YAP	$+ P_{FDH1}\_FDH(V9)_{Pse}$	
PpCβ21-PE	$+ P_{DAS1}\_ESBP6_{Sc}$	
PpCβ21-PJ	$+ P_{DAS2}\_JEN1$	
PpCβ21-PEJ	$+ P_{DAS2}\_JEN1$	
PpCβ21-PEJY	$+ P_{SHB17}\_PYC2$	
PpCβ21-PEJΔfdh1	$+ FDH1^{-}$	
PpCβ21-PEJYΔfdh1	$+ FDH1^{-}$	

to increase NADPH availability further improved both methanol consumption (q_S) and specific productivity (q_P) rates in strain PpCβ21-P. Despite our demonstration of the potential of *K. phaffii* for 3-HP production from renewable C1 feedstocks, the obtained yield and productivity fell short of the commercially feasible metrics. Typically, minimum values of 0.5 g g^{-1} and 2.5 g l^{-1} h^{-1}, respectively, are required to develop an economically viable bioprocess for carboxylic acid production [8, 40].

Besides increasing NADPH availability, other strategies have been investigated to improve 3-HP yield in engineered yeast harboring the β-alanine pathway. In particular, improvement of the supply of the β-alanine pathway's metabolic precursors in *S. cerevisiae* has been demonstrated to have a significant positive impact on 3-HP production [23]. This was achieved by overexpressing the *AAT2*, *PYC1* and *PYC2* genes, encoding enzymes catalyzing the conversion of pyruvate into aspartate, the precursor of this synthetic pathway.

Another engineering strategy commonly used in yeast/ fungi to enhance organic acid production is the overexpression of genes encoding membrane transporters to facilitate final product export [41, 42]. To date, no 3-HP-specific transporters have been identified in yeast. However, given that lactate and 3-HP are structural isomers, some studies have focused on existing lactate transporters as potential candidates for 3-HP export. In *S. cerevisiae*, two monocarboxylate permeases have been identified, Esbp6 [43] and Jen1 [44]. Esbp6, also known as Mch3, may play a role in acid-stress adaptation responses, as well as in functions related to cell wall integrity maintenance. *K. phaffii*'s genome has a potential ORF annotated as *ESBP6* (GenBank accession number CAH2449939). However, it has not been experimentally characterized, and its function remains unknown. Overexpression of *ESBP6* in the plasma membrane of an engineered *S. cerevisiae* strain improved lactic acid production by 20% under non-neutralizing conditions, probably due to enhanced lactic acid tolerance [45]. Similarly, Qin et al. [46] demonstrated that deleting *ESBP6* in a wild-type strain cultivated in the presence of 50 g l^{-1} 3-HP at pH 3.5 inhibited growth considerably, whereas *ESBP6* overexpression significantly increased cell tolerance to 3-HP compared to the wild-type strain. The lactate-proton symporter Jen1 can mediate the electroneutral transport of lactic acid when it accumulates inside the cell [29]. In fact, overexpression of Jen1 has been shown to improve lactic acid production in recombinant *S. cerevisiae* strains [47–50]. This effect has also been observed in the non-conventional yeast *K. phaffii* by Lima et al. [51], who identified a *JEN1* ortholog in the *K. phaffii* genome showing 50.19% identity to the *S. cerevisiae*'s *JEN1* gene. Overexpression of the gene encoding this putative lactate transporter in a recombinant *K. phaffii*

strain producing L-lactic acid from glycerol resulted in a 46% increase in lactate yield compared to the control strain.

In this study, we further optimized our previously developed 3-HP-producing strains [39] by implementing a range of metabolic engineering strategies. First, efforts were focused on a "push" strategy aiming at increasing the supply of intermediates of the β-alanine pathway, i.e. oxaloacetate and aspartate, and to further channel flux through the heterologous NADP-dependent formate dehydrogenase by deleting the *FDH1* gene encoding the endogenous NAD-dependent analogous enzyme. Second, using a "pull" strategy, we sought to promote 3-HP export by overexpressing the endogenous *JEN1* gene and the *ESBP6* gene from *S. cerevisiae*. Notably, the latter strategy resulted in a substantial increase in 3-HP productivity. Both strategies were tested individually and in a combined way. Moreover, we characterized the resulting strains at pH 3.5, an industrially relevant condition for carboxylic acid production.

Materials and methods
Plasmid and strain construction
The parental strains *K. phaffii* PpCβ21 and PpCβ21-P [39] were used as platform chassis to construct a new generation of strains with optimized metabolic pathway towards 3-HP production and exportation. Homology-directed integrations of heterologous genes and knockout of the endogenous *FDH1* coding sequence were performed using CRISPR/Cas9 technology. Plasmids and strains constructed in this study are listed in Table 1. Further description of the molecular biology workflow followed in this study can be found in Additional file 1.

Following the CRISPR/Cas9-mediated genome editing protocol in *K. phaffii*, two sgRNAs were individually designed and generated for each locus to target (Table 2) and inserted into the BB3cN_p*GAP*_23*_pLAT1_Cas9 plasmid from the CRIS*Pi* kit [52]. Potential sgRNA

candidates binding target regions within the selected loci were assessed with CHOPCHOP [53], as described in Àvila-Cabré et al. [39]. Shortly, the highest-scoring protospacers (20-nucleotide target sites followed by a PAM sequence) identified by CHOPCHOP were chosen for sgRNAs design. Additionally, two secondary criteria were considered: avoiding the presence of four consecutive thymine bases (TTTT) and aiming for a GC content of 20–80% (excluding the PAM sequence), as outlined by Yang et al. [54].

Electrocompetent *K. phaffii* cells were prepared as described elsewhere [55]. Co-transformation of the donor DNA template and the BB3 plasmid harboring the sgRNA and a human codon optimized Cas9 for episomal expression in *K. phaffii* was performed as described in Gassler et al. [52].

Most of the genomic regions for CRISPR/Cas9-mediated integration of expression cassettes were selected based on previous studies showing stable expression and unaffected cell fitness [56, 57], focusing on intergenic regions such as upstream or downstream of promoters or terminators, respectively (Table 2). The *AAT2* and Asp-DH$_{Spe}$ expression cassettes were individually targeted into an intergenic region located 250-bp upstream of P$_{ENO1}$ (PP7435_Chr3-1154). *PYC2* expression unit was located 600-bp downstream of *AOX1tt* (PP7435_Chr4-0131). *JEN1* and *ESBP6*$_{Sc}$ heterologous cassettes were initially targeted right after *GUT1tt* (PP7435_Chr4-0174). However, no positive transformants were found after several attempts. Alternatively, these expression cassettes were individually targeted to PP7435_Chr3-1154 in strains that did not harbor *AAT2*/AspDH$_{Spe}$ overexpression. When co-expressing both monocarboxylate permeases, *ESBP6*$_{Sc}$ was targeted to PP7435_Chr3-1154, while *JEN1* was located into an intergenic region 1000-bp upstream of P$_{OPT1-1}$ (PP7435_Chr4-1011). Finally, the FDH(V9)$_{Pse}$ expression cassette was targeted within 50-bp upstream of P$_{AOX1}$ (PP7435_Chr4-0130) [39].

Table 2 Variable sgRNA targets custom-designed in this study

Target name	Locus	Sequence (5' ◊ 3')	Module inserted
p*ENO1*^{UP}_sgRNA1	PP7435_Chr3-1154	**TTATTGAAGATACCGCCCGG**	P$_{DAS1}$-*AAT2*-*RPS3*tt
			P$_{DAS1}$-AspDH$_{Spe}$-*RPS3*tt
p*ENO1*^{UP}_sgRNA2		**CGTTTAAACTTACCTCCGGG**	P$_{DAS2}$-*JEN1*- Sc*CYC1*tt
			P$_{DAS1}$-*ESBP6*$_{Sc}$- Sc*CYC1*tt
*AOX1*tt$_{DOWN}$_sgRNA1	PP7435_Chr4-0131	**ACTATTGATCCAAGCCAGTG**	P$_{SHB17}$-*PYC2*-*RPS3*tt
*AOX1*tt$_{DOWN}$_sgRNA2		GCTGATTTGGGGTTTAATAC	
*GUT1*tt$_{DOWN}$_sgRNA1	PP7435_Chr4-0174	**GGTAGATGAGTTATTAACTG**	P$_{DAS2}$-*JEN1*-Sc*CYC1*tt
*GUT1*tt$_{DOWN}$_sgRNA2		**AAACTGCGAATAAGAAAGCA**	P$_{DAS1}$-*ESBP6*$_{Sc}$-Sc*CYC1*tt
p*OPT1-1*^{UP}_sgRNA1	PP7435_Chr4-1011	ACTAACCAGAGCAAACACTG	P$_{DAS2}$-*JEN1*-Sc*CYC1*tt
p*AOX1*^{UP}_sgRNA1	PP7435_Chr4-0130	**ATTGTGAAATAGACGCAGAT**	P$_{FDH1}$-FDH(V9)$_{Pse}$-*TDH3*tt
p*AOX1*^{UP}_sgRNA2		GCAGTCGATCTCAAAAGCAA	
Δ*FDH1*_sgRNA1	PP7435_Chr3-0238	ATCGGCGGCGTGCTTACCAG	-
Δ*FDH1*_sgRNA2		**GTTCTCGTTTTGTACTCCGC**	

The sgRNA target used for each genomic insertion is highlighted in bold

Correct genomic insertions from three individual transformants from each strain were checked at both 5' and 3' ends of the integrated donor DNA by Sanger sequencing.

The *K. phaffii FDH1* gene (PP7435_Chr3-0238) was disrupted using insertions or deletions (InDel) mutations by expressing a BB3 vector containing both a sgRNA and Cas9. The resulting double-strand break (DSB) in the genomic DNA occurred 25–32 base pairs from the *FDH1* start, depending on the specific sgRNA used (Table 2). The disrupted locus was verified by Sanger sequencing. The sequencing was performed by the Genomics and Bioinformatics Service of the Universitat Autònoma de Barcelona.

Recombinant yeast strains were grown at 30 °C in YPD-agar plates (1% yeast extract, 2% peptone, 2% dextrose and 15 g l^{-1} agar). The medium was supplemented with Nourseothricin (200 µg ml^{-1} working concentration for *K. phaffii*) from Dismed S.A. (Asturias, Spain).

Screening in deep-well plates

Three clones of every *K. phaffii* strain were inoculated into 50-ml falcon tubes containing 5 ml of YPG medium (1% yeast extract, 2% peptone and 1% v/v glycerol) and grown overnight at 30 °C and 180 rpm in an incubator shaker Multitron Standard from Infors HT (Bottmingen, Switzerland) with a 2.5 cm orbit. Overnight cultures were inoculated in triplicate at a starting OD_{600} of 0.1 into 24-deep-well plates containing 2 ml of buffered minimal methanol medium (BMM; 100 mM potassium phosphate buffer pH 6, 1.34% yeast nitrogen base (YNB), 0.4 mg l^{-1} biotin and 0.5% v/v pure methanol). Cultures were incubated at 25 °C and 220 rpm in the same incubator shaker. The deep-well plates were placed on a platform with a slope of 20° to improve aeration. Relative humidity (rh) in the incubation chamber was fixed to 80%. After 24 h, 1% v/v pure methanol pulse (7.9 g l^{-1}) was added to each well. Cultures were grown for 48 h to ensure full consumption of the substrate.

At the end of the culture, the endpoint OD_{600} of each well was measured in duplicate with a 96-well microtiter plate using a Multiskan FC Microplate Photometer from Thermo Fisher Scientific (Waltham, MA, USA). Thereafter, culture samples were collected into 2-ml microcentrifuge tubes and centrifuged at 13,400 rpm for 5 min using a MiniSpin from Eppendorf (Hamburg, Germany). Supernatant was then filtered with a 0.2-µm pore size single-use syringe filter (SLLGX13NK) from Merck Millipore (Burlington, MA, USA). 3-HP and methanol were quantified from the filtered supernatant by HPLC analysis. Raw datasets of small-scale cultivations are provided in Additional file 2.

Bioreactor cultivations

For the bioreactor cultivations, the batch medium consisted of 40 g l^{-1} glycerol, 1.8 g l^{-1} citric acid, 0.02 g l^{-1} $CaCl_2 \cdot 2H_2O$, 12.6 g l^{-1} $(NH_4)_2HPO_4$, 0.5 g l^{-1} $MgSO_4 \cdot 7H_2O$, 0.9 g l^{-1} KCl, 50 µl antifoam Glanapon 2000 kz (Bussetti and Co GmbH, Vienna, Austria), 0.4 mg l^{-1} biotin, 2 ml l^{-1} of vitamin stock solution [58], and 5 ml l^{-1} of PTM1 trace salts [59]. The pH was adjusted to 5 using 5 M HCl. The vitamins, the biotin and the trace salts were filter-sterilized and added to the bioreactors after cooling down.

Fed-batch cultures were performed in duplicate using a DASGIP Parallel Bioreactor System from Eppendorf (Hamburg, Germany). Reactors were inoculated at a starting OD_{600} equal to 1, and the initial volume was 500 ml. The pH was controlled at 5 throughout the culture using 15% ammonia. The temperature was set to 28 °C during the batch phase. The inlet gas was fed into the reactors at an aeration rate of 1 vvm (0.5 l min^{-1}). The dissolved oxygen (DO) was set to 30%. The agitation gradually increased from 400 to 1,000 rpm to maintain DO set point. When agitation reached 1,000 rpm, pure oxygen was mixed with air in the inlet gas to maintain a pO_2 above 30%, while maintaining an aeration rate of 0.5 l min^{-1}. For the fed-batch phase, the temperature was set to 25 °C. Pure methanol ($\rho = 792$ g l^{-1}) and feeding salts were added separately to the culture to avoid precipitation. The feeding salts medium composition was 0.35 g l^{-1} $CaCl_2 \cdot 2H_2O$, 10 g l^{-1} KCl, 6.45 g l^{-1} $MgSO_4 \cdot 7H_2O$, 200 µl antifoam Glanapon 2000 kz, 1.2 mg l^{-1} biotin, 6 ml l^{-1} of vitamin stock solution, and 15 ml l^{-1} of PTM1 trace salts. This media was prepared at 2× concentration since pure methanol was used. The vitamins, the biotin, and the trace salts were filter-sterilized and added to this final feeding solution.

At the end of the glycerol batch phase (glycerol depletion indicated by spike in the dissolved oxygen tension and verified by HPLC at the start of the methanol feed phase), two consecutive pulses of pure methanol (1 and 2 g l^{-1}, respectively) were added to the reactors. Once methanol was fully depleted, the cultures were fed with a constant methanol feed (F_o) to complete the transition phase. For cultivations at pH 3.5, the pH set point was adjusted from 5 to 3.5 at the start of the second stage of the transition phase (i.e. during the constant methanol feed), allowing the pH to gradually decrease over the following hours (see Additional file 3). After that, the feeding medium was added to the bioreactors using a pre-programmed exponential feeding strategy for controlled specific growth rate described in the following equation:

$$F(t) = \frac{\mu\,[X(t_o)\,V(t_o)]}{Y_{X/S}\,S_o}e^{[\mu\,(t-t_o)]}$$

where growth rate (μ) was set to 0.03 h^{-1}, initial biomass concentration (X_0) was fixed at 22 g l^{-1}, biomass yield ($Y_{X/S}$) was 0.273 g g^{-1}, and initial substrate concentration (S_o) was 792 g l^{-1}.

The reactors were sampled during 39 h to measure OD_{600}, biomass dry cell weight (DCW), and supernatant metabolites. DCW was determined gravimetrically in triplicate using paper filters. A volume of 10 ml of a 9 g l^{-1} NaCl solution was used to wet the pre-weighed glass microfiber filters (APFF04700) from Merck Millipore (Burlington, MA, USA) before filtering 2 ml of culture for each triplicate. Filters were subsequently washed using the same volume of NaCl solution, dried for 24 h at 105 °C, and weighed to calculate the DCW. To quantify glycerol, methanol and 3-HP, 2 ml of culture samples were centrifuged 5 min at 13,400 rpm using a MiniSpin (Eppendorf, Germany), and the supernatant was filtered with a 0.2-µm pore size single-use syringe filter (SLL-GX13NK, Merck Millipore).

Raw datasets and calculations of growth and 3-HP production parameters of bioreactor cultivations are shown in Additional file 4.

Analytical methods and data processing

Methanol and 3-HP were quantified using an HPLC Ultimate3000 from Dionex (Thermo Fischer Scientific, Waltham, MA, USA) equipped with an ionic exchange column ICSep ICE-COREGEL 87H3 from Transgenomic (Omaha, NE, USA) and a Refractive Index detector. The mobile phase consisted of 6 mM sulphuric acid with a flow rate of 0.6 ml min^{-1}.

The OD_{600} measurements were performed in triplicate using a Lange DR 3900 spectrophotometer from Hach (Loveland, CO, USA). Analytical replicates were averaged, and the standard deviation (SD) was calculated for each OD_{600} determination. Biomass (dry cell weight, DCW) was determined in triplicate for three samples throughout the fed-batch. For the rest of the samples, the biomass DCW values were calculated from the measured OD_{600} values, based on the calibration curve made for the given strain.

Offline and online state variables —such as biomass (X), substrate (S), product (P), flow rate (F), and initial volume (V_o)— were recorded during the fed-batch phase of the bioreactor-scale experiments (see Additional files 3 and 4). These variables were used to calculate derived metrics, including growth rate (μ), q-rates, and yields, following the methodology described elsewhere [39]. For mass balance verification, the elemental biomass composition $CH_{1.88}O_{0.63}N_{0.20}S_{0.004}$ was assumed, based on cells growing on methanol at $\mu = 0.035$ h^{-1} [60]. Carbon and electron balances were satisfied with a deviation of less than 7%. A statistical χ^2 consistency test, based on the h-index, was applied to the measured data balances [61, 62], following the detailed method described by Ponte et al. [63]. The consistency tests passed with a confidence level of 95%, confirming no major measurement errors.

Computational methods

The genome-scale metabolic model iMT1026 v3.0 of *K. phaffii* [60] was employed to calculate the theoretical maximum 3-HP yield ($\Upsilon_{3-HP\ max}$) achievable on methanol via the β-alanine pathway under different growth conditions. This model was expanded to include 3-HP production and excretion reactions. Simulations were constrained using experimental values obtained for the key physiological macroscopic parameters μ and q_S, derived from methanol fed-batch cultivations. Specifically, μ was set to 0.028 h^{-1} and q_S was 0.109 g_{MetOH} g_{DCW}^{-1} h^{-1} (Table 3). Additionally, the $\Upsilon_{3-HP\ max}$ was calculated under non-growth conditions ($\mu = 0$ h^{-1}). The non-growth associated maintenance energy (NGAME) parameter for methanol growth from Tomàs-Gamisans et al. [60] was also applied as a constraint. Flux Balance Analysis (FBA) was performed in COBRA Toolbox v3.0 [64] with Matlab R2021a (Mathworks, Inc., Natick, MA, USA) to maximize specific 3-HP productivity (q_P) as the objective function. Finally, q_P values resulting from the FBA, together with the experimental q_S, were used to determine the $\Upsilon_{3-HP\ max}$.

Table 3 Average values of key production parameters obtained from the exponential methanol feed phase of fed-batch cultivations using a pre-programmed μ of 0.03 h^{-1}. Volumetric productivity (Q_P), biomass yield on methanol ($Y_{X/S}$), 3-HP yield on methanol ($Y_{P/S}$), 3-HP yield on biomass ($Y_{P/X}$), CO_2 yield on methanol ($Y_{CO2/S}$), specific substrate consumption rate (q_S), specific 3-HP production rate (q_P), specific carbon dioxide evolution rate (q_{CO2}), and experimentally measured mean specific growth rate (μ). Cultivations were performed in duplicate and biomass concentration analyses were performed in triplicate. ± indicates SD of the biological replicates

	PpCβ21-P	PpCβ21-PEJY
Q_P (g_{3-HP} l^{-1} h^{-1})	0.46 ± 0.01	0.56 ± 0.03
$Y_{X/S}$ (g_{DCW} g_{MetOH}^{-1})	0.21 ± 0.01	0.25 ± 0.01
$Y_{P/S}$ (g_{3-HP} g_{MetOH}^{-1})	0.15 ± 0.01	0.19 ± 0.01
$Y_{P/X}$ (g_{3-HP} g_{DCW}^{-1})	0.69 ± 0.03	0.74 ± 0.02
$Y_{CO2/S}$ (g_{CO2} g_{MetOH}^{-1})	0.81 ± 0.03	0.68 ± 0.02
q_S (g_{MetOH} g_{DCW}^{-1} h^{-1})	0.124 ± 0.003	0.109 ± 0.001
q_P ($mmol_{3-HP}$ g_{DCW}^{-1} h^{-1})	0.201 ± 0.008	0.227 ± 0.006
q_{CO2} ($mmol_{CO2}$ g_{DCW}^{-1} h^{-1})	2.30 ± 0.08	1.69 ± 0.04
μ (h^{-1})	0.026 ± 0.001	0.028 ± 0.001
Reference	[39]	This study

Results and discussion

Engineering precursor supply of the β-alanine pathway for 3-HP production

To enhance pyruvate flux to aspartate, the precursor of the β-alanine pathway, we individually overexpressed native genes encoding the pyruvate carboxylase isoform 2 (*PYC2*), which catalyzes the ATP-dependent carboxylation of pyruvate to form OAA, and the cytosolic aspartate aminotransferase 2 (*AAT2*), which enables the conversion of OAA to aspartate by transferring an amino group from glutamate (Fig. 1). These genes were overexpressed in the original strain PpCβ21 [39] by integrating a second copy of the corresponding coding sequence under the control of methanol-inducible promoters into the *K. phaffii* genome. The expression of *AAT2* in strain PpCβ21-A was driven by the strong dihydroxyacetone synthase 1 promoter (P_{DAS1}), while *PYC2* in strain PpCβ21-Y was expressed under the control of the medium-strength sedoheptulose bisphosphatase promoter (P_{SHB17}) to avoid additional disturbances in the central metabolic node of pyruvate. Additionally, a highly active and stable NAD- or NADP-dependent aspartate dehydrogenase from *Serratia proteamaculans* (SpeAspDH) [65], which directly aminates OAA using ammonium as the amino donor, was tested as an alternative to *K. phaffii AAT2* under P_{DAS1}, resulting in strain PpCβ21-D strain (Fig. 1).

None of the individually overexpressed genes led to a significant improvement in final 3-HP concentration or yield on methanol ($Y_{P/S}$) after 48 h of cultivation in 24-deep-well plates with BMM medium, except in the case of *PYC2* overexpression (strain PpCβ21-Y),
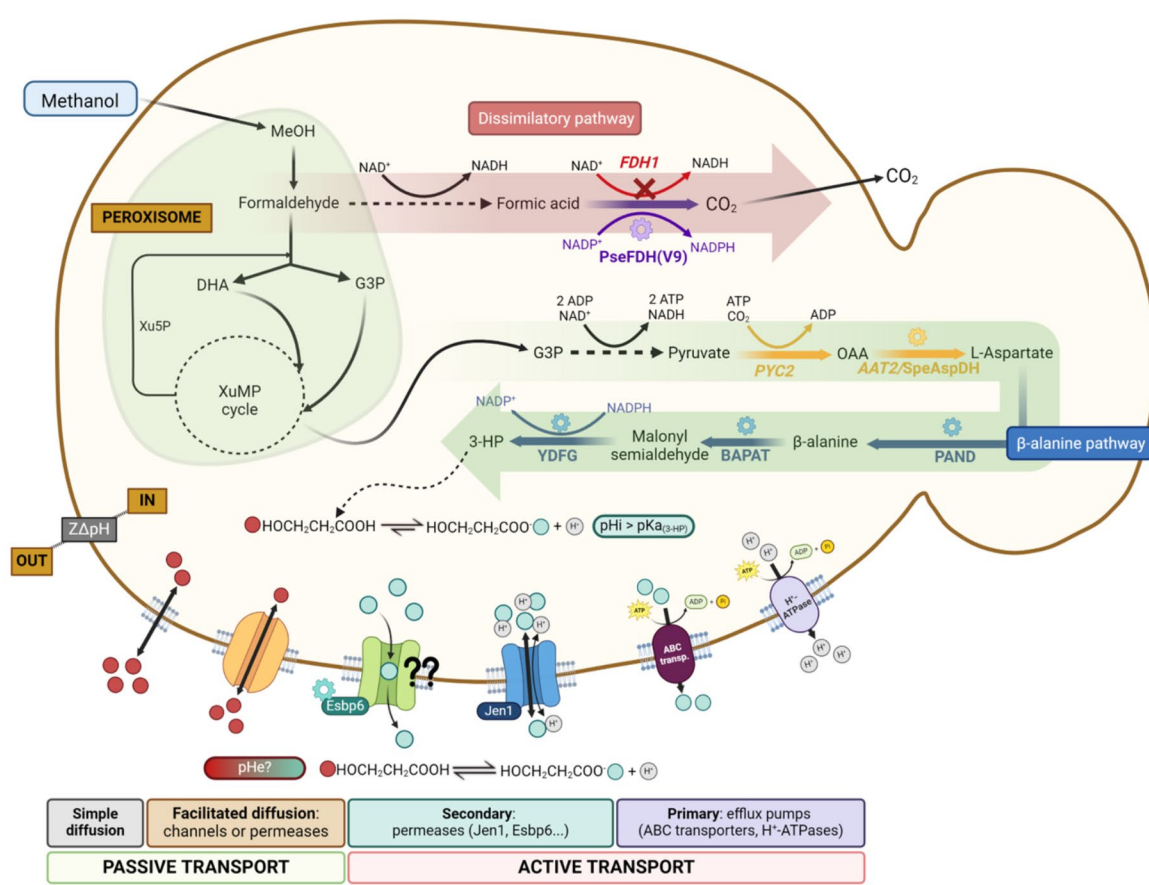
Fig. 1 Schematic representation of methanol metabolism, 3-HP production via the β-alanine pathway, and carboxylic acids transport mechanisms reported in yeast. The pathway of 3-HP synthesis is shaded in green; and the methanol dissimilatory pathway is shaded in red. Heterologous enzymes are indicated with colored gears. While uncharged 3-HP ($HOCH_2CH_2COOH$) can passively diffuse across the plasma membrane, its anionic form ($HOCH_2CH_2COO^-$) is hypothesized to require active transport via ABC transporters or permeases (i.e., Jen1 symporter). Dissociation of 3-HP in the cytosol releases protons (H^+), which are mainly extruded by H^+-ATPases, maintaining pH balance and electrochemical potential across the membrane (ZΔpH) [70]. *FDH1*, NAD-dependent formate dehydrogenase; PseFDH(V9), mutated NADP-dependent formate dehydrogenase; *PYC2*, pyruvate carboxylase isoform 2; *AAT2*, aspartate aminotransferase 2; SpeAspDH, NAD- or NADP-dependent aspartate dehydrogenase; PAND, aspartate-1-decarboxylase; BAPAT, β-alanine-pyruvate aminotransferase; YDFG, 3-hydroxypropionate dehydrogenase

which resulted in a slight but statistically significant 5.4% increment ($p = 0.03$) in the 3HP yield on biomass ($Y_{P/X}$), increasing from 0.556 to 0.586 g l^{-1} of 3-HP per OD_{600} unit compared to the reference strain (PpCb21). We hypothesize that the modest increase in 3-HP yields could be due to an insufficient ATP supply, as the carboxylation of pyruvate by Pyc2 enzyme is ATP-dependent [66]. Additionally, bicarbonate, a co-substrate in this carboxylation reaction, might also become a rate-limiting factor in these strains [46, 67].

Neither *AAT2* nor the *S. proteamaculans* AspDH's encoding gene overexpression did improve 3-HP production, suggesting that the conversion of OAA into aspartate may not be a rate-limiting step of the 3-HP pathway. These findings are consistent with those from a previous study involving a recombinant *K. phaffii* strain that converted methanol into β-alanine, in which overexpression of either mitochondrial *AAT1* or cytosolic *AAT2* did not significantly enhance β-alanine production [65]. Coherently, engineering the entire upstream module of the β-alanine pathway, i.e., co-overexpression of an additional copy of both *PYC2* and *AAT2*, resulting in strain PpCβ21-YA, did not lead to significant improvements in $Y_{P/S}$ and $Y_{P/X}$ compared to the PpCβ21-Y strain ($p = 0.58$ and 0.30, respectively).

Further engineering attempts to boost the precursors supply of the β-alanine pathway included the overexpression of a mutated NADP-dependent formate dehydrogenase from *Pseudomonas* sp. 101, PseFDH(V9), aiming at enhancing NADPH supply of this pathway (Fig. 1). In a previous study, PseFDH(V9) overexpression in the PpCβ21 reference strain, generating the PpCβ21-P strain, resulted in a 14% and 10% increase in $Y_{P/X}$ and q_P, respectively, as well as higher q_s in methanol fed-batch cultivations, despite performing poorly in 24-deep-well plates [39]. Similarly, introduction of PseFDH(V9) coding gene under the control of the formate dehydrogenase promoter (P_{FDH1}) in strain PpCβ21-YA, creating strain PpCβ21-YAP, decreased 3-HP titers by 11% ($p = 0.0017$) in 24-deep-well plate cultures. Nevertheless, based on the observed enhanced performance of PpCβ21-P in bioreactor-scale cultivations, we considered this strain as a base strain for further metabolic engineering for 3-HP production.

Overexpression of monocarboxylate permeases encoding genes leads to higher 3-HP production

Overexpression of the genes encoding the synthetic β-alanine pathway combined with higher *PYC2* expression levels may lead to 3-HP accumulation in the cytosol. Owing to the near-neutral pH of the cytoplasm, 3-HP dissociates at the time of being produced, releasing protons and anions that poorly diffuse to extracellular space.

Therefore, high intracellular 3-HP concentrations are likely to have a negative effect on cell metabolism.

To maintain intracellular pH (pHi) homeostasis, (an) ions must be actively exported through different free energy-dependent processes such as: (i) primary transport, via ATP-Binding Cassette (ABC) transporters and plasma membrane H$^+$-ATPases, and (ii) secondary transport, via transporters that use (electro-)chemical gradients as the driving force (e.g., Jen1 symporter) (Fig. 1). To date, no specific ABC transporters have been identified for 3-HP export.

In this study, the *JEN1* and *ESBP6* genes encoding putative monocarboxylate permeases were individually introduced into the PpCβ21-P strain [39], under the control of strong methanol-inducible promoters, resulting in strains PpCβ21-PJ and PpCβ21-PE, respectively. After 48 h of cultivation in BMM medium in 24-deep-well plates, the highest concentration of 3-HP (1.40 ± 0.04 g l^{-1}) was obtained with strain PpCβ21-PE, resulting in a 44% increase in both titer and yields compared to the reference strain (Fig. 2). Notably, although PpCβ21-PE produced a higher amount of 3-HP than PpCβ21-P, both strains reached similar biomass levels. While the function of Esbp6 remains unknown [43], overexpression of its gene clearly enhanced 3-HP titer and yields in the recombinant strain PpCβ21-PE. These results are consistent with findings from other studies [45, 46], where overexpression of *ESBP6* improved yeast tolerance to acid-stressing conditions by reducing the intracellular 3-HP content, ultimately leading to a higher 3-HP production.

Conversely, overexpression of *JEN1* in strain PpCβ21-PJ led to modest yet statistically significant increase of 8% in $Y_{P/S}$ and 12% in $Y_{P/X}$ ($p = 0.0008$ and 0.044, respectively) compared to PpCβ21-P (Fig. 2), suggesting that Jen1 may have a lower export efficiency or capacity for 3-HP compared to Esbp6. Further characterization of these transporters could provide insights into the distinct effects on 3-HP export observed in this study.

Interestingly, disruption of the endogenous *JEN1* gene in a *S. cerevisiae* 3-HP-producing strain did not result in significant differences in the final 3-HP concentration compared to the parental strain, indicating that 3-HP efflux in the Δ*jen1* strain remained functional [46]. Similar results were observed in *S. cerevisiae* strains producing lactic acid, where Δ*jen1* strains, and even isogenic yeast mutants Δ*jen1*Δ*ady2*, showed no differences in lactic acid production compared to the wild-type strain, suggesting the presence of other lactic acid exporters besides Jen1 [48, 49]. However, Lima et al. [51] reported a 46% increase in lactate yield when *JEN1* was overexpressed in a recombinant *K. phaffii* strain. Therefore, it is also plausible that the limited impact of *JEN1* overexpression in strain PpCβ21-PJ might be due to the lower
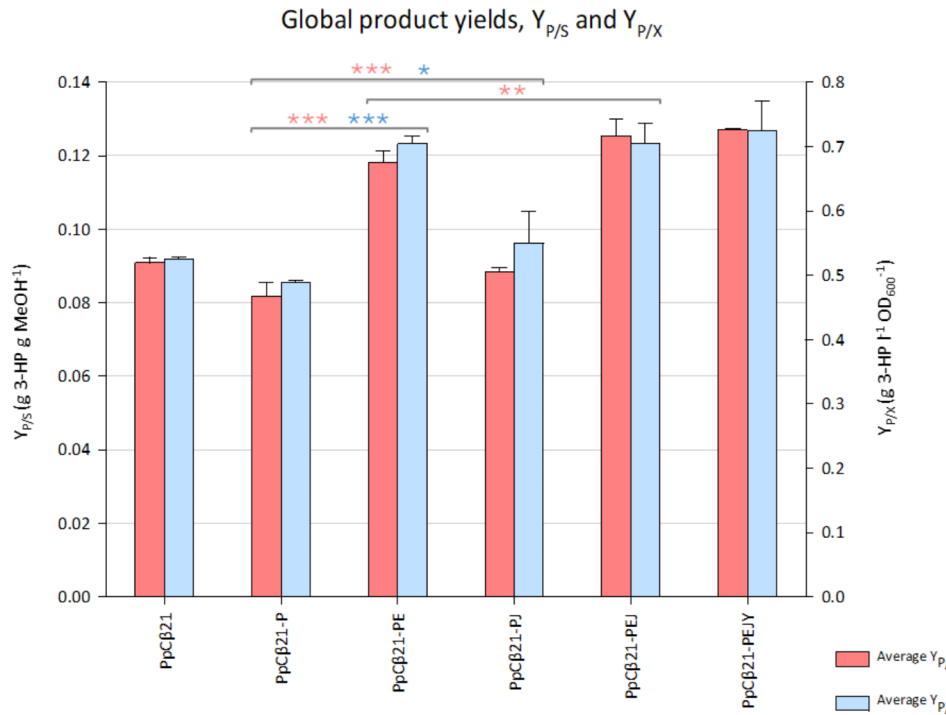
Fig. 2 Average global product yields calculated for the strains constructed in this study, $Y_{P/S}$ and $Y_{P/X}$. The salmon-colored bars show the average 3-HP yield on methanol ($g_{3\text{-HP}}$ g_{MeOH}^{-1}), while light blue was used for bars representing the average 3-HP yield on biomass ($g_{3\text{-HP}}$ OD_{600} unit^{-1}). The error bars show the standard deviation. Significant differences between two groups are shown in the graph. Statistical analysis was conducted using a two-tailed unpaired Student's t-test (*p < 0.05, **p < 0.01, ***p < 0.001)

affinity of this putative lactate transporter for 3-HP anions compared to lactate.

When *JEN1* and *ESBP6* were overexpressed simultaneously in strain PpCβ21-PEJ, the $Y_{P/X}$ was similar to that of *ESBP6* overexpression alone, while the $Y_{P/S}$ showed a modest but significant increase of 6% ($p = 0.001$), rising from 0.118 g g^{-1} in strain PpCβ21-PE to 0.125 g g^{-1} (Fig. 2). These findings corroborate that the monocarboxylate transporters, particularly Esbp6, effectively facilitated the export of 3-HP *in K. phaffii*.

Finally, to combine "push" and "pull" metabolic engineering strategies, a second copy of the *K. phaffii PYC2* gene was integrated into the PpCβ21-PEJ genome, aiming to enhance metabolic precursors supply to the β-alanine pathway, resulting in strain PpCβ21-PEJY. However, this strain did not show significant changes in $Y_{P/S}$ and $Y_{P/X}$ compared to PpCβ21-PEJ when grown in 24-deep-well plates, with *p*-values of 0.34 and 0.31, respectively.

Overall, strains PpCβ21-PEJ and PpCβ21-PEJY showed the highest improvements in both $Y_{P/S}$ (53 and 55%, respectively) and $Y_{P/X}$ (44 and 48%) compared to the reference strain PpCβ21-P (Fig. 2). As a result, both strains were taken for further evaluation in bioreactors.

Production of 3-HP in fed-batch cultivations
Strains PpCβ21-PEJ and PpCβ21-PEJY were further characterized in bioreactor-scale fed-batch cultivations

consisting of three phases, i.e. an initial glycerol batch phase for biomass production (at the end of which glycerol was depleted), followed by a transition phase including two pulses of methanol and a 6-h constant methanol feed to adapt cells to methanolic conditions, and a final methanol-feed phase of about 40 h for 3-HP production using a pre-programmed exponential methanol feeding strategy at a growth rate of $\mu = 0.02$ h^{-1}. At the start of the exponential methanol feed phase biomass and 3-HP levels were 21 g l^{-1} and 5 g l^{-1}, respectively. Both strains reached a 3-HP concentration of 24.6 g l^{-1} and nearly identical biomass levels (38.0 and 37.8 g l^{-1}, respectively) at the end of the process. Approximately 70 g of methanol were added during the exponential feed phase of the respective cultivations, yielding a 3-HP yield on methanol ($Y_{P/S}$) of 0.20 g g^{-1} for both strains. Residual methanol was not detected by HPLC analysis over the course of fermentation.

Given that both PpCβ21-PEJ and PpCβ21-PEJY strains performed similarly, one of them, strain PpCβ21-PEJY, was further tested in an analogous fed-batch cultivation process where the exponential methanol feed phase was adjusted at a $\mu_{SP} = 0.03$ h^{-1}, i.e. under the same conditions used for characterization of our original strains [39]. During this phase, 3-HP augmented from 5 g l^{-1} to 27.0 ± 0.4 g l^{-1}. This represents a 42% increase in 3-HP titer compared to the parental strain PpCβ21-P cultivated

under the same conditions (Fig. 3), which is consistent with results observed in small-scale experiments. These findings corroborate that lactate transporters, such as Esbp6 and Jen1, effectively facilitate 3-HP export.

Interestingly, strain PpCβ21-PEJY significantly decreased the CO_2 yield on methanol ($Y_{CO2/S}$) from 0.81 (strain PpCβ21-P) to 0.68 g_{CO2} g_{MetOH}^{-1} ($p = 0.01$), while both $Y_{P/S}$ and $Y_{X/S}$ were significantly increased by 27 and 19%, respectively (Table 3) ($p = 0.04$ and 0.01). A plausible explanation for this observation may be that the increased export of 3-HP caused by the overexpression of monocarboxylate permeases in the PpCβ21-PEJY strain, particularly Esbp6, seems to provoke a metabolic "pull" effect, draining a higher proportion of the incoming methanol flux towards the assimilatory pathway, thereby favoring 3-HP production and biomass synthesis, while reducing CO_2 generation through the dissimilatory methanol oxidation pathway.

A global $Y_{P/S}$ of 0.17 C-mol C-mol^{-1} was obtained when considering both glycerol and methanol cultivation phases, while a $Y_{P/S}$ of 0.20 C-mol C-mol^{-1} was calculated for the exponential methanol feeding phase. These yields are comparable to that of our top-performing *K. phaffii* strain engineered with the malonyl-CoA pathway for 3-HP production on glycerol (0.19 C-mol C-mol^{-1}) [21]. This finding is particularly significant considering that the $\Upsilon_{3-HP\ max}$ achievable on methanol is considerably lower than on C-sources such as glucose or glycerol, assuming all carbon is used solely for 3-HP synthesis ($\mu = 0$ h^{-1}) [39]. The yield achieved here corresponds to 70% of the $\Upsilon_{3-HP\ max}$ under biomass-generating conditions (0.27 g_{3-HP} g_{MetOH}^{-1}), i.e., reflecting the specific growth rate in our fed-batch experiments. Coherently, the $\Upsilon_{3-HP\ max}$ is considerably higher when all carbon is exclusively channeled toward 3-HP production, with no biomass generation (0.78 g_{3-HP} g_{MetOH}^{-1}). Under these conditions, our experimental $Y_{P/S}$ represents 24.4% of this theoretical yield (see Materials and Methods section). Strain PpCβ21-PEJY also demonstrated over a 20% improvement in volumetric productivity (Q_P) compared to the reference strain (Table 3). Notably, a recent study using an extensively engineered *K. phaffii* strain harboring the malonyl-CoA reductase pathway has reported a
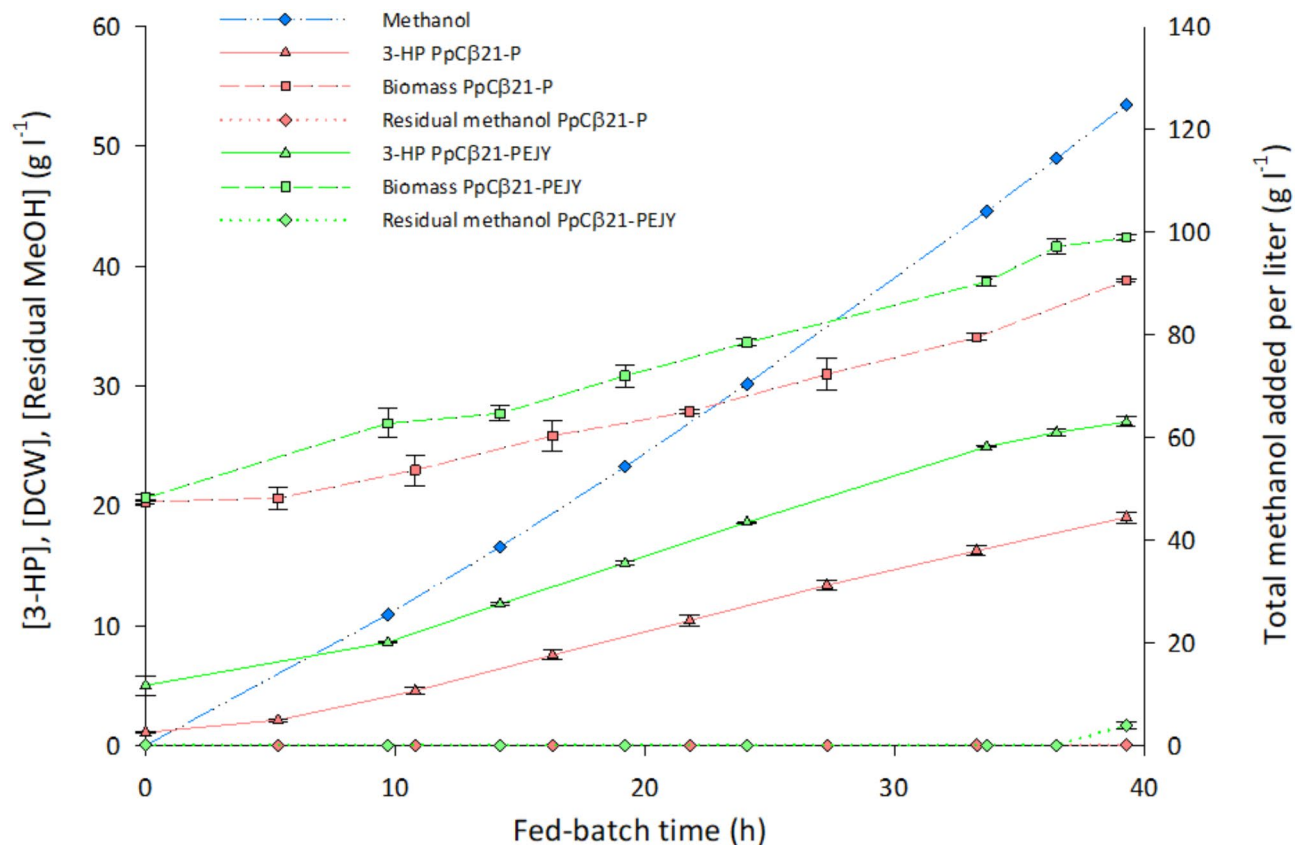

Fig. 3 Fed-batch phase profiles from the bioreactor-scale experiments with PpCβ21-P and PpCβ21-PEJY strains at pH 5. Concentrations of dry cell weight, 3-HP, and residual methanol are represented in the left-side y-axis. The total amount of methanol added, normalized by the actual volume of the reactor at every time, is represented using the right-side y-axis. Time axis corresponds to the exponential methanol feeding phase of the cultivations (preprogrammed at a μ = 0.03 h^{-1}). The cultivation profile shown for each strain corresponds to the average result of two independent cultivations. The error bars denote the standard deviation for the duplicate
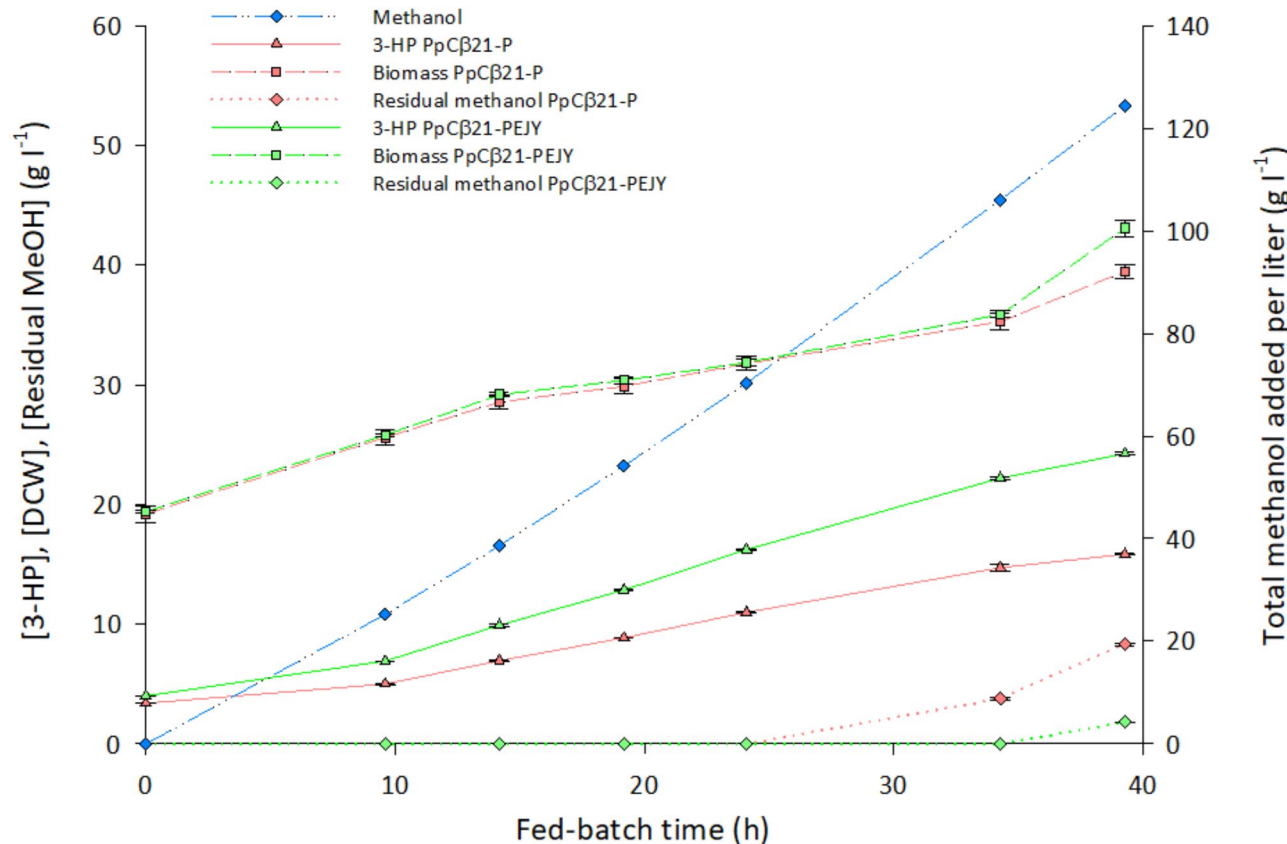
Fig. 4 Fed-batch phase profiles from the bioreactor-scale experiments with PpCβ21-P and PpCβ21-PEJY strains at pH 3.5. Concentrations of dry cell weight, 3-HP, and residual methanol are represented in the left-side y-axis. The total amount of methanol added is represented using the right-side y-axis. Time axis corresponds to the exponential methanol feeding phase of the cultivations (preprogrammed at a $\mu = 0.03$ h^{-1}). Data represent a single cultivation replicate for each strain. The error bars denote the standard deviation of triplicate measurements for each sample

3-HP yield on methanol slightly higher than in our study (0.23 g g^{-1}) [38].

ESBP6 and *JEN1* overexpression improves strain robustness at pH 3.5

Production of 3-HP at a low pH would allow for a more economical downstream processing, while reducing the risk of bacterial contamination. For instance, acidification is not needed for product recovery, effectively reducing costs. Furthermore, the amounts of base titrant required for neutralization during fermentation are greatly decreased at low pH, especially at industrial scale [8, 29].

To evaluate if differences exist in terms of tolerance to acidic conditions between the reference and the engineered strains overexpressing the lactate transporters encoding genes, production of 3-HP with strains PpCβ21-P and PpCβ21-PEJY was also tested in fed-batch cultures at pH 3.5, following the same strategy used for their initial characterization at pH 5.

Both PpCβ21-P and PpCβ21-PEJY strains produced 3-HP at acidic pH, achieving final titers of 15.9 ± 0.1 g l^{-1} and 24.2 ± 0.1 g l^{-1}, respectively (Fig. 4). As expected, strain PpCβ21-PEJY outperformed PpCβ21-P also at

lower pH values. It is known that the energy demands of product export could hinder 3-HP production, particularly if the metabolic pathway involved has little to no net ATP yield [29]. Accordingly, the two tested strains produced lower 3-HP yields on methanol at pH 3.5 compared to pH 5. However, while strain PpCβ21-P produced 3-HP at a yield of 0.11 g g^{-1} at pH 3.5, that is, a decrease of 26.7% compared to the yield at pH 5, strain PpCβ21-PEJY achieved a 3-HP yield of 0.17 g g^{-1} at low pH, that is, just 10.5% decrease from that obtained at pH 5 (0.19 g g^{-1}). These findings are coherent with earlier research on 3-HP synthesis by *S. cerevisiae* [23] and *K. phaffii* cultivated under pH 3.5 conditions [68].

Under such acidic conditions, the undissociated fraction of 3-HP is the predominant form in the solution. Particularly at high concentrations, uncharged 3-HP may cross the cell membrane through either simple diffusion or facilitated diffusion (via a channel or a permease). Once in the cytoplasm, neutral pH leads to dissociation of the 3-HP acid, releasing protons and anions (Fig. 1). The released protons may cause cytosolic acidification, which is harmful to the cell, whereas anions may trigger the generation of free radicals, resulting in severe

oxidative stress [69, 70]. Hence, to maintain pH homeostasis in the cytosol, active transport mechanisms, which require metabolic energy, allow for exporting these accumulated (an)ions from the cytosol. The lower 3-HP yields achieved at pH 3.5 compared to pH 5 may reflect this increased ATP demand, underscoring ATP as a limiting factor in 3-HP production, consistent with previous findings [68]. Nevertheless, overexpression of genes encoding monocarboxylate transporters, especially *ESBP6*, effectively facilitated the export of anionic 3-HP in strain PpCβ21-PEJY. This could explain why the lower pH had a reduced effect on the 3-HP yield of strain PpCβ21-PEJY compared to strain PpCβ21-P.

Interestingly, both strains PpCβ21-P and PpCβ21-PEJY reached comparable levels of biomass concentration in cultures at the two pH values (Figs. 3 and 4), suggesting that acidic pH had no impact on biomass yields. However, studies investigating carboxylic acid production in *S. cerevisiae* [71] and *K. phaffii* [68] found contrasting results, linking reduced biomass yields to increased maintenance-energy requirements in such conditions.

Knockout of the endogenous NAD-dependent formate dehydrogenase encoding gene (*FDH*1) to reduce carbon loss through the methanol dissimilatory pathway reveals limited efficiency of the heterologous NADP-dependent formate dehydrogenase

Despite the essential role of the methanol dissimilatory pathway in formaldehyde detoxification and energy production, it leads to a huge loss of carbon atoms through CO_2 release [72].

The combination of different metabolic engineering strategies described so far resulted in a shift of carbon flux from the dissimilatory pathway towards 3-HP production. Strain PpCβ21-PEJY, which overexpresses a mutated NADP-dependent formate dehydrogenase (PseFDH(V9)), two monocarboxylate transporters (Esbp6 and Jen1), and pyruvate carboxylase isoform 2 (Pyc2), showed a 16% reduction in CO_2 yield and a 27% increase in 3-HP yield in methanol fed-batch cultures compared to the parental strain (Table 3).

To further decrease CO_2 formation, the *K. phaffii FDH1* endogenous gene, encoding a NAD-dependent formate dehydrogenase, was deleted in strains PpCβ21-PEJ and PpCβ21-PEJY, resulting in strains PpCβ21-PEJΔ*fdh1* and PpCβ21-PEJYΔ*fdh1*, respectively. This strategy aimed to channel formate oxidation to CO_2 exclusively through the NADP-dependent PseFDH(V9) (Fig. 1).

Strains PpCβ21-PEJΔ*fdh1* and PpCβ21-PEJYΔ*fdh1* were cultivated in triplicate alongside their parental strains in 24-deep-well plates containing BMM medium. Both 3-HP production and cell growth were drastically reduced by over 90% compared to their respective parental strains (see Additional file 2). This suggests that

NADH generated from dissimilated formaldehyde via *FLD* was not sufficient to make up for the loss of NADH (and consequently, ATP) typically produced by native *FDH*, leading to an energy imbalance and suboptimal growth on methanol. Notably, around 1 g l^{-1} of formic acid (FA) accumulated at the end of the cultivation, indicating that PseFDH(V9) activity alone was not enough to fully oxidize FA to CO_2, creating a bottleneck in the dissimilatory pathway. The accumulation of toxic intermediates, such as FA (and formaldehyde), likely contributed to the impaired growth observed, also supporting the proposed physiological role of *FDH* in formate detoxification rather than in energy production [73]. Moreover, partial blocking of the dissimilatory pathway also led to up to 4.3 g l^{-1} of residual methanol, suggesting additional metabolic bottlenecks downstream the methanol assimilatory pathway.

Similar challenges were reported by Guo et al. [35] when the methanol dissimilation pathway was completely blocked through *FDH* deletion in a *K. phaffii* strain engineered to produce malic acid from methanol. In contrast, a recent study found no significant growth differences between a *K. phaffii* GS115 strain and an *FDH*-deficient GS115 strain grown on 1% YPM, suggesting context-dependent effects of *FDH* deletion on methanol metabolism. Moreover, comparative transcriptomic analysis revealed that the impact of *FDH* deletion was less pronounced than that caused by the deletion of other genes involved in the methanol dissimilatory pathway (*FLD*, *FGH*) [74].

Conclusions

In this study, we enhanced the performance of our previously developed 3-HP-producing strains through several metabolic engineering strategies focusing on the improvement of yields and productivities. These strategies included: (i) overexpressing the upstream module of the β-alanine pathway, (ii) partially blocking the methanol dissimilation pathway, and (iii) reducing intracellular 3-HP accumulation. To our knowledge, this is the first time the *S. cerevisiae*'s gene encoding the lactate transporter Esbp6 has been expressed in *K. phaffii*, proving its effectiveness in facilitating 3-HP export. Overall, co-overexpression of *ESBP6* and *JEN1*, encoding two lactate transporters, along with *PYC2* to enhance oxaloacetate supply, led to a total 3-HP concentration of 27.0 g l^{-1}, with a product yield of 0.19 g g^{-1} and a volumetric productivity of 0.56 g l^{-1} h^{-1} for the exponential methanol feeding phase. However, deleting *FDH1* in *K. phaffii* impaired growth, probably due to an energy imbalance or poor performance of the heterologous PseFDH(V9).

Notably, we further demonstrated 3-HP production under industrially relevant cultivation conditions, specifically at a low pH of 3.5, and highlighted the beneficial

effects of overexpressing genes encoding lactate transporters, such as Esbp6 and Jen1, to support 3-HP production at pH 3.5.

While this work highlights the potential of using efficient monocarboxylate transporters to achieve high productivities, yields, and titers of the target carboxylic acid, further improvements are needed to reach industrially relevant metrics. Furthermore, a deeper understanding of the export mechanisms, substrate specificity, and regulation of carboxylate transporters is crucial for the successful development of microbial cell factories for industrial carboxylic acid production, regardless of the pH conditions used in the fermentation processes.

Advancements in the field of metabolic engineering [75] are paving the way for *K. phaffii* to emerge as a relevant industrial cell factory for 3-HP production from methanol. Improving the efficiency of methanol assimilation and metabolic network-wide analysis to investigate the optimality of energy and redox metabolism under 3-HP overproducing conditions should guide the development of efficient chassis strains, taking also into account pathway compartmentalization [25, 76].

Supplementary Information

The online version contains supplementary material available at https://doi.org/10.1186/s13036-025-00488-x.

Supplementary Material 1: **Additional file 1**: Molecular cloning materials and methods. The file contains Table S1: List of primers used in this study.

Supplementary Material 2: **Additional file 2**: Raw data from the 24-deep-well plate cultivations. The file includes raw HPLC and OD_{600} data, quantification of metabolites, product yields determination, and statistical analyses.

Supplementary Material 3: **Additional file 3**: Raw data of the online monitored standard process parameters. The file also contains two charts representing the evolution of key process parameters (DO, pH, T and outlet gas CO_2) throughout fed-batch cultivations of strain PpCβ21-PEJY at pH 5 and 3.5.

Supplementary Material 4: **Additional file 4**: Raw and processed data obtained from bioreactor-scale experiments. The file includes raw HPLC and biomass data, quantification of metabolites and biomass concentrations, averaged values for key physiological and production parameters from fed-batch cultures, and statistical analyses.

Author contributions
SAC, JA, and PF conceived and designed the research project. SAC performed all experiments and analyzed the data. PF and JA contributed to data interpretation and discussion. SAC wrote the first draft of the manuscript and PF contributed to the manuscript final version. All authors read and approved the final manuscript.

Data availability
Data is provided within the manuscript or supplementary information files. Further raw datasets used and/or analyzed during the current study are available from the corresponding author on reasonable request https://doi.org/10.34810/data1807.

Declarations

Ethics approval and consent to participate
Not applicable.

Consent for publication
Not applicable.

Competing interests
The authors declare no competing interests.

Author details
¹Department of Chemical, Biological and Environmental Engineering, Universitat Autònoma de Barcelona, Cerdanyola del Vallès, Barcelona, Catalonia, Spain

References
1. Olah GA. Beyond oil and gas: the methanol economy. Angew Chem Int Ed. 2005;44:2636–9.
2. Sarwar A, Lee EY. Methanol-based biomanufacturing of fuels and chemicals using native and synthetic methylotrophs. Synth Syst Biotechnol. 2023;8:396–415.
3. Bachleitner S, Ata Ö, Mattanovich D. The potential of CO_2-based production cycles in biotechnology to fight the climate crisis. Nat Commun. 2023;14:6978.
4. Vásquez Castro E, Memari G, Ata Ö, Mattanovich D. Carbon efficient production of chemicals with yeasts. Yeast. 2023;40:583–93.
5. Lv X, Yu W, Zhang C, Ning P, Li J, Liu Y, Du G, Liu L. C1-based biomanufacturing: advances, challenges and perspectives. Bioresour Technol. 2023;367:128259.
6. Jiang X, Meng X, Xian M. Biosynthetic pathways for 3-hydroxypropionic acid production. Appl Microbiol Biotechnol. 2009;82:995–1003.
7. Rathnasingh C, Raj SM, Jo JE, Park S. Development and evaluation of efficient recombinant *Escherichia coli* strains for the production of 3-hydroxypropionic acid from glycerol. Biotechnol Bioeng. 2009;104:729–39.
8. Werpy T, Petersen G. Top value added chemicals from biomass: volume I — results of screening for potential candidates from sugars and synthesis gas. Springfield (VA): US Department of Energy; 2004. Report No. DOE/GO-102004-1992.
9. Bozell JJ, Petersen GR. Technology development for the production of biobased products from biorefinery carbohydrates—the US Department of Energy's top 10 revisited. Green Chem. 2010;12:539–55.
10. Della Pina C, Falletta E, Rossi M. A green approach to chemical building blocks. The case of 3-hydroxypropanoic acid. Green Chem. 2011;13:1624–32.
11. Kumar V, Ashok S, Park S. Recent advances in biological production of 3-hydroxypropionic acid. Biotechnol Adv. 2013;31:945–61.
12. de Fouchécour F, Sánchez-Castañeda AK, Saulou-Bérion C, Spinnler HÉ. Process engineering for microbial production of 3-hydroxypropionic acid. Biotechnol Adv. 2018;36:1207–22.
13. Jers C, Kalantari A, Garg A, Mijakovic I. Production of 3-hydroxypropanoic acid from glycerol by metabolically engineered bacteria. Front Bioeng Biotechnol. 2019;7:124.
14. Kim JW, Ko YS, Chae TU, Lee SY. High-level production of 3-hydroxypropionic acid from glycerol as a sole carbon source using metabolically engineered *Escherichia coli*. Biotechnol Bioeng. 2020;117:2139–52.

15. Zhao P, Ma C, Xu L, Tian P. Exploiting tandem repetitive promoters for high-level production of 3-hydroxypropionic acid. Appl Microbiol Biotechnol. 2019;103:4017–31.
16. Ji RY, Ding Y, Shi TQ, Lin L, Huang H, Gao Z, Ji XJ. Metabolic engineering of yeast for the production of 3-hydroxypropionic acid. Front Microbiol. 2018;9:2185.
17. Kildegaard KR, Jensen NB, Schneider K, Czarnotta E, Özdemir E, Klein T, Maury J, Ebert BE, Christensen HB, Chen Y, Kim IK, Herrgård MJ, Blank LM, Forster J, Nielsen J, Borodina I. Engineering and systems-level analysis of *Saccharomyces cerevisiae* for production of 3-hydroxypropionic acid via malonyl-CoA reductase-dependent pathway. Microb Cell Fact. 2016;15:53.
18. Yu W, Cao X, Gao J, Zhou YJ. Overproduction of 3-hydroxypropionate in a super yeast chassis. Bioresour Technol. 2022;361:127690.
19. Suyama A, Higuchi Y, Urushihara M, Maeda Y, Takegawa K. Production of 3-hydroxypropionic acid via the malonyl-CoA pathway using recombinant fission yeast strains. J Biosci Bioeng. 2017;124:392–9.
20. Takayama S, Ozaki A, Konishi R, Otomo C, Kishida M, Hirata Y, Matsumoto T, Tanaka T, Kondo A. Enhancing 3-hydroxypropionic acid production in combination with sugar supply engineering by cell surface-display and metabolic engineering of *Schizosaccharomyces Pombe*. Microb Cell Fact. 2018;17:176.
21. Fina A, Heux S, Albiol J, Ferrer P. Combining metabolic engineering and multiplexed screening methods for 3-hydroxyprionic acid production in *Pichia pastoris*. Front Bioeng Biotechnol. 2022;10:942304.
22. Kildegaard KR, Wang Z, Chen Y, Nielsen J, Borodina I. Production of 3-hydroxypropionic acid from glucose and xylose by metabolically engineered *Saccharomyces cerevisiae*. Metab Eng Commun. 2015;2:132–6.
23. Borodina I, Kildegaard KR, Jensen NB, Blicher TH, Maury J, Sherstyk S, Schneider K, Lamosa P, Herrgård MJ, Rosenstand I, Öberg F, Forster J, Nielsen J. Establishing a synthetic pathway for high-level production of 3-hydroxypropionic acid in *Saccharomyces cerevisiae* via β-alanine. Metab Eng. 2015;27:57–64.
24. Lis AV, Schneider K, Weber J, Keasling JD, Jensen MK, Klein T. Exploring small-scale chemostats to scale up microbial processes: 3-hydroxypropionic acid production in *S. Cerevisiae*. Microb Cell Fact. 2019;18:50.
25. Boob AG, Tan SI, Zaidi A, Singh N, Xue X, Zhou S, Martin TA, Chen LQ, Zhao H. Design of diverse, functional mitochondrial targeting sequences across eukaryotic organisms using variational autoencoder. BioRxiv. 2024; *preprint under review*.
26. Kayalvizhi R, Sanjana J, Jacob S, Kumar V. An eclectic review on dicarboxylic acid production through yeast cell factories and its industrial prominence. Curr Microbiol. 2024;81:147.
27. Wang Y, Wang Y, Cui J, Wu C, Yu B, Wang L. Non-conventional yeasts: promising cell factories for organic acid bioproduction. Trends Biotechnol. 2025. https://doi.org/10.1016/j.tibtech.2024.12.004. online ahead of print.
28. Budavari S. The Merck index: an encyclopedia of chemicals, drugs, and biologicals. 11th ed. Rahway: Merck; 1989.
29. van Maris AJ, Konings WN, Dijken JPV, Pronk JT. Microbial export of lactic and 3-hydroxypropanoic acid: implications for industrial fermentation processes. Metab Eng. 2004;6:245–55.
30. Guo F, Qiao Y, Xin F, Zhang W, Jiang M. Bioconversion of C1 feedstocks for chemical production using *Pichia pastoris*. Trends Biotechnol. 2023;41:1066–79.
31. Liu XB, Liu M, Tao XY, Zhang ZX, Wang FQ, Wei DZ. Metabolic engineering of *Pichia pastoris* for the production of dammarenediol-II. J Biotechnol. 2015;216:47–55.
32. Gao J, Zuo Y, Xiao F, Wang Y, Li D, Xu J, Ye C, Feng L, Jiang L, Liu T, Gao D, Ma B, Huang L, Xu Z, Lian J. Biosynthesis of catharanthine in engineered *Pichia pastoris*. Nat Synth. 2023;2:231–42.
33. Cai P, Li Y, Zhai X, Yao L, Ma X, Jia L, Zhou YJ. Microbial synthesis of long-chain α-alkenes from methanol by engineering *Pichia pastoris*. Bioresour Bioprocess. 2022;9:58.
34. Cai P, Wu X, Deng J, Gao L, Shen Y, Yao L, Zhou YJ. Methanol biotransformation toward high-level production of fatty acid derivatives by engineering the industrial yeast *Pichia pastoris*. Proc Natl Acad Sci U S A. 2022;119:e2201711119.
35. Guo F, Dai Z, Peng W, Zhang S, Zhou J, Ma J, Dong W, Xin F, Zhang W, Jiang M. Metabolic engineering of *Pichia pastoris* for malic acid production from methanol. Biotechnol Bioeng. 2021;118:357–71.
36. Yamada R, Ogura K, Kimoto Y, Ogino H. Toward the construction of a technology platform for chemicals production from methanol: D-lactic acid production from methanol by an engineered yeast *Pichia pastoris*. World J Microbiol Biotechnol. 2019;35:37.
37. Severinsen MM, Bachleitner S, Modenese V, Ata Ö, Mattanovich D. Efficient production of itaconic acid from the single-carbon substrate methanol with engineered *Komagataella Phaffii*. Biotechnol Biofuels Bioprod. 2024;17:98.
38. Wu X, Cai P, Gao L, Li Y, Yao L, Zhou YJ. Efficient bioproduction of 3-hydroxypropionic acid from methanol by a synthetic yeast cell factory. ACS Sustain Chem Eng. 2023;11:6445–53.
39. Àvila-Cabré S, Pérez-Trujillo M, Albiol J, Ferrer P. Engineering the synthetic β-alanine pathway in *Komagataella phaffii* for conversion of methanol into 3-hydroxypropionic acid. Microb Cell Fact. 2023;22:237. Erratum in Microb Cell Fact. 2024;23:235.
40. Mazzoli R. Current progress in production of building-block organic acids by consolidated bioprocessing of lignocellulose. Fermentation. 2021;7:248.
41. Soares-Silva I, Ribas D, Sousa-Silva M, Azevedo-Silva J, Rendulić T, Casal M. Membrane transporters in the bioproduction of organic acids: state of the art and future perspectives for industrial applications. FEMS Microbiol Lett. 2020;367:fnaa118.
42. Wu T, Li J, Tian C. Fungal carboxylate transporters: recent manipulations and applications. Appl Microbiol Biotechnol. 2023;107:5909–22.
43. Makuc J, Paiva S, Schauen M, Krämer R, André B, Casal M, Leão C, Boles E. The putative monocarboxylate permeases of the yeast *Saccharomyces cerevisiae* do not transport monocarboxylic acids across the plasma membrane. Yeast. 2001;18:1131–43.
44. Casal M, Paiva S, Andrade RP, Gancedo C. The lactate-proton symport of *Saccharomyces cerevisiae* is encoded by *JEN1*. J Bacteriol. 1999;181:2620–3.
45. Sugiyama M, Akase S, pei, Nakanishi R, Kaneko Y, Harashima S. Overexpression of *ESBP6* improves lactic acid resistance and production in *Saccharomyces cerevisiae*. J Biosci Bioeng. 2016;122:415–20.
46. Qin N, Li L, Wan X, Ji X, Chen Y, Li C, Liu P, Zhang Y, Yang W, Jiang J, Xia J, Shi S, Tan T, Nielsen J, Chen Y, Liu Z. Increased CO_2 fixation enables high carbon-yield production of 3-hydroxypropionic acid in yeast. Nat Commun. 2024;15:1591.
47. Porro D, Bianchi M, Ranzi B, Frontali L, Vai M, Winkler A, Alberghina L. Yeast strains for the production of lactic acid. Patent WO1999014335A1; 1999.
48. Branduardi P, Sauer M, De Gioia L, Zampella G, Valli M, Mattanovich D, Porro D. Lactate production yield from engineered yeasts is dependent from the host background, the lactate dehydrogenase source and the lactate export. Microb Cell Fact. 2006;5:4.
49. Pacheco A, Talaia G, Sá-Pessoa J, Bessa D, Gonçalves MJ, Moreira R, Paiva S, Casal M, Queirós O. Lactic acid production in *Saccharomyces cerevisiae* is modulated by expression of the monocarboxylate transporters Jen1 and Ady2. FEMS Yeast Res. 2012;12:375–81.
50. Zhu P, Luo R, Li Y, Chen X. Metabolic engineering and adaptive evolution for efficient production of L-lactic acid in *Saccharomyces cerevisiae*. Microbiol Spectr. 2022;10:e0227722.
51. Lima PBA, Mulder KCL, Melo NTM, Carvalho LS, Menino GS, Mulinari E, de Castro VH, Dos Reis TF, Goldman GH, Magalhães BS, Parachin NS. Novel homologous lactate transporter improves L-lactic acid production from glycerol in recombinant strains of *Pichia pastoris*. Microb Cell Fact. 2016;15:158.
52. Gassler T, Heistinger L, Mattanovich D, Gasser B, Prielhofer R. CRISPR/Cas9-mediated homology-directed genome editing in *Pichia pastoris*. Methods Mol Biol. 2019;1923:211–25.
53. Labun K, Montague TG, Gagnon JA, Thyme SB, Valen E. CHOPCHOP v2: a web tool for the next generation of CRISPR genome engineering. Nucleic Acids Res. 2016;44:W272–6.
54. Yang Y, Liu G, Chen X, Liu M, Zhan C, Liu X, Bai Z. High efficiency CRISPR/Cas9 genome editing system with an eliminable episomal sgRNA plasmid in *Pichia pastoris*. Enzyme Microb Technol. 2020;138:109556.
55. Sears IB, O'connor J, Rossanese OW, Glick BS. A versatile set of vectors for constitutive and regulated gene expression in *Pichia pastoris*. Yeast. 1998;14:783–90.
56. Liu Q, Shi X, Song L, Liu H, Zhou X, Wang Q, Zhang Y, Cai M. CRISPR—Cas9-mediated genomic multiloci integration in *Pichia pastoris*. Microb Cell Fact. 2019;18:144.
57. Prielhofer R, Barrero JJ, Steuer S, Gassler T, Zahrl R, Baumann K, Sauer M, Mattanovich D, Gasser B, Marx H. GoldenPiCS: a Golden Gate-derived modular cloning system for applied synthetic biology in the yeast *Pichia pastoris*. BMC Syst Biol. 2017;11:123.
58. Jensen NB, Strucko T, Kildegaard KR, David F, Maury J, Mortensen UH, Forster J, Nielsen J, Borodina I. EasyClone: method for iterative chromosomal integration of multiple genes in *Saccharomyces cerevisiae*. FEMS Yeast Res. 2014;14:238–48.

59. Maurer M, Kühleitner M, Gasser B, Mattanovich D. Versatile modeling and optimization of fed batch processes for the production of secreted heterologous proteins with *Pichia pastoris*. Microb Cell Fact. 2006;5:37.

60. Tomàs-Gamisans M, Ferrer P, Albiol J. Fine-tuning the *P. pastoris* iMT1026 genome-scale metabolic model for improved prediction of growth on methanol or glycerol as sole carbon sources. Microb Biotechnol. 2018;11:224–37.

61. Noorman HJ, Rornein B, Ch M, Luyben KA, Heijnen JJ. Classification, error detection, and reconciliation of process information in complex biochemical systems. Biotechnol Bioeng. 1996;49:364–76.

62. van der Heijden RT, Heijnen JJ, Hellinga C, Romein B, Luyben KC. Linear constraint relations in biochemical reaction systems: I. classification of the calculability and the balanceability of conversion rates. Biotechnol Bioeng. 1994;43:3–10.

63. Ponte X, Montesinos-Seguí JL, Valero F. Bioprocess efficiency in *Rhizopus oryzae* lipase production by *Pichia pastoris* under the control of P$_{AOX1}$ is oxygen tension dependent. Process Biochem. 2016;51:1954–63.

64. Becker SA, Feist AM, Mo ML, Hannum G, Palsson B, Herrgard MJ. Quantitative prediction of cellular metabolism with constraint-based models: the COBRA Toolbox. Nat Protoc. 2007;2:727–38.

65. Miao L, Li Y, Zhu T. Metabolic engineering of methylotrophic *Pichia pastoris* for the production of β-alanine. Bioresour Bioprocess. 2021;8:89.

66. Tong T, Tao Z, Chen X, Gao C, Liu H, Wang X, Liu GQ, Liu L. A biosynthesis pathway for 3-hydroxypropionic acid production in genetically engineered *Saccharomyces cerevisiae*. Green Chem. 2021;23:4502–9.

67. Malubhoy Z, Bahia FM, de Valk SC, de Hulster E, Rendulić T, Ortiz JPR, Xiberras J, Klein M, Mans R, Nevoigt E. Carbon dioxide fixation via production of succinic acid from glycerol in engineered *Saccharomyces cerevisiae*. Microb Cell Fact. 2022;21:102.

68. Fina A, Millard P, Albiol J, Ferrer P, Heux S. High throughput ^{13}C-metabolic flux analysis of 3-hydroxypropionic acid producing *Pichia pastoris* reveals limited availability of acetyl-CoA and ATP due to tight control of the glycolytic flux. Microb Cell Fact. 2023;22:117.

69. Peetermans A, Foulquié-Moreno MR, Thevelein JM. Mechanisms underlying lactic acid tolerance and its influence on lactic acid production in *Saccharomyces cerevisiae*. Microb Cell. 2021;8:111–30.

70. Piper P, Calderon CO, Hatzixanthis K, Mollapour M. Weak acid adaptation: the stress response that confers yeasts with resistance to organic acid food preservatives. Microbiol (Reading). 2001;147:2635–42.

71. Hakkaart X, Liu Y, Hulst M, el Masoudi A, Peuscher E, Pronk J, et al. Physiological responses of *Saccharomyces cerevisiae* to industrially relevant conditions: slow growth, low pH, and high CO$_2$ levels. Biotechnol Bioeng. 2020;117:721–35.

72. Yurimoto H, Kato N, Sakai Y. Assimilation, dissimilation, and detoxification of formaldehyde, a central metabolic intermediate of methylotrophic metabolism. Chem Rec. 2005;5:367–75.

73. Sakai Y, Murdanoto AP, Konishi T, Iwamatsu A, Kato N. Regulation of the formate dehydrogenase gene, *FDH1*, in the methylotrophic yeast *Candida boidinii* and growth characteristics of an *FDH1*-disrupted strain on methanol, methylamine, and choline. J Bacteriol. 1997;179:4480–5.

74. Yu YF, Yang J, Zhao F, Lin Y, Han S. Comparative transcriptome and metabolome analyses reveal the methanol dissimilation pathway of *Pichia pastoris*. BMC Genomics. 2022;23:366.

75. Volk MJ, Tran VG, Tan SI, Mishra S, Fatma Z, Boob A, Li H, Xue P, Martin TA, Zhao H. Metabolic engineering: methodologies and applications. Chem Rev. 2023;123:5521–70.

76. Fina A, Àvila-Cabré S, Vázquez-Pereira E, Albiol J, Ferrer P. A rewired NADPH-dependent redox shuttle for testing peroxisomal compartmentalization of synthetic metabolic pathways in *Komagataella Phaffii*. Microorganisms. 2025;13:46.

Publisher's note